MEASURING THE NORMAL SPECTRAL INFRARED EMISSIVITY OF STRUCTURAL MATERIALS

L. N. Aksyutov, A. K. Pavlyukov,
and G. K. Kholopov

UDC 536.3

The emissivity of various structural materials was measured over the 2-10 μm range of wavelengths at temperatures from 50 to 200°C; the results are shown and their accuracy is evaluated.

The measurement of directional and, particularly, the normal spectral emissivity is of most interest where scientific and technical applications are concerned. With the value of this coefficient known, it is possible, for instance, to calculate the normal total emissivity [1] (the validity of such a calculation has been confirmed experimentally in [2]) and from this the hemispherical total emissivity [3]. Data on the spectral emissivity of materials at temperatures below 500°C are extremely scarce, however. Furthermore, the proposed methods of measurement have not been perfected yet and this presents an obstacle to their wider application in the evaluation of various materials with different properties. In order to make measurements by the method shown in [4], for example, the specimen must be shaped into a cylinder with a narrow slot in the wall. The dependence of test data on the ambient radiation determines the lowest specimen temperature, which should not be lower than 200°C. Two methods of measuring the spectral emissivity at lower temperatures have been proposed in [5]. Their gist is that, in order to eliminate the effect of ambient radiation, the measurements are made with a self-contained black body (at several slightly different temperatures) and with a system comprising two specimens and two black-body models pairwise at two different temperatures. The application of these methods evades the effect of ambient radiation, to be sure, but it also complicates the measurement procedure appreciably without eliminating the need for precise measurement and maintenance of the temperatures of both the specimens and the black-body models. In [6] the authors have proposed a procedure for measuring the normal spectral emissivity of opaque materials by means of two standard specimens, a "white" one and a "black" one, at the same temperature as the test specimen.

In this article we present the results of emissivity measurements pertaining to various structural materials, within the 2-10 μm range of wavelengths and at temperatures from 50 to 200°C, with a subsequent evaluation of their accuracy.

As has been shown in [6], the normal spectral emissivity of a specimen is determined according to the formula:

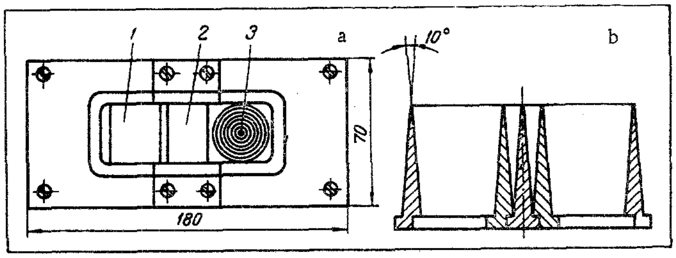

Fig. 1. Layout of standard specimens and test specimen in the heated yoke.

Translated from Inzhenerno-Fizicheskii Zhurnal, Vol. 24, No. 3, pp. 393-399, March, 1973. Original article submitted April 20, 1972.

$$\varepsilon(\lambda, T) = \varepsilon_{bl}(\lambda, T)\frac{N - N_{wh}}{N_{bl} - N_{wh}} + \varepsilon_{bl}(\lambda, T)\frac{N_{bl} - N}{N_{bl} - N_{wh}}. \tag{1}$$

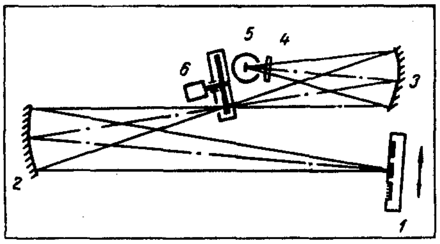

Fig. 2. Layout of the measuring apparatus.

The standards and the test specimen are put in a heatable yoke, the latter having been designed so as to ensure that all specimens are at the same temperature. The location of all specimens on the front side of the yoke is shown in the dimensioned diagram in Fig. 1a: here item 1 is the "white" standard, item 2 is the test specimen, and item 3 is the "black" standard. For the "white" standard we used a gold disc with a smoothly polished surface. It is common knowledge [7] that gold is one of the metals almost perfectly resistant to oxidation in air when heated to rather high temperatures. The data on the spectral emissivity of gold were taken from [8]. For the "black" standard we used a model of an ideal black body, an assembly of rings of various diameters shown in cross section in Fig. 1b.

The surface temperature of the solid copper disc, heated in the yoke together with the test specimen and the other standard specimen, was measured with a platinum resistance thermometer as one arm of a model MVU-49 dc bridge circuit. The disc surface was scanned by the pad of a receiver-probe, to check whether the temperature distribution here remained uniform. This was ascertained by a constant output signal from that receiver-probe. The radiation receiver was a cooled (51°K) Ge–Hg photoresistor for the 2-10 μm wavelengths and an uncooled PbS photoresistor for the 1-3 μm wavelengths. The measuring apparatus is shown schematically in Fig. 2. A test specimen inside the heated yoke 1 was emitting radiation in the direction normal to its surface and this radiation was collected by a spherical mirror 2 (f = 300 mm, D = 150 mm), from there transmitted to another spherical mirror 3 (f = 500 mm, D = 210 mm), which then focused it on the pad of receiver 5. The yoke, the mirrors, and the receiver were positioned so that the receiver pad 1 mm in diameter would project on the specimen surface magnified 3-4 times. The radiation was made monochromatic by means of optical interference filters 4 with a 40-60% transmittivity and a relative pass-bandwidth $\Delta\lambda/\lambda_{max} = 0.05 \pm 0.01$ for the following peak-transmission wavelengths λ_{max} = 1.80, 1.93, 2.12, 2.66, 3.30, 3.66, 3.85, 4.30, 4.68, 5.10, 6.13, 6.75, 7.66, 8.47, and 9.30 μm. The radiation was modulated at a frequency of 600 Hz. The modulator blades were enveloped by a shroud whose inside surface had been coated with soot. The output signals from the receiver were preamplified by a model V6-2 selective microvoltmeter and then recorded by a model V7-8 voltmeter.

We will now analyze the basic sources of errors, which determine the accuracy of measurements [6].

1. Imperfection of the Ideal-Black-Body Model. It is well known that the emissivity of a cavity depends on its shape and also on the degree of its nonisothermality. The emissivity of the ideal-black-body model made up of rings was calculated here on the basis of assuming very thin ring elements, relative to their radii. On this basis, the analog of our ideal-black-body model was an infinitely long groove of triangular cross section with a 10° vertex angle. The spectral emissivity of points on the wall surface of such a groove at a distance x_0 from the vertex and at a temperature T_{x_0} was not much different from the vertex temperature T (operating temperature of the model) and was determined according to the formula which the authors had derived for diffuse reflection from groove walls with a spectral reflectivity $\rho \ll 1$:

$$\varepsilon_{x_0}(\lambda) = (1-\rho)\left\{1 + \frac{\rho}{2}\left[1 + \frac{\cos\alpha - x_0}{\sqrt{1 + x_0^2 - 2x_0\cos\alpha}}\right]\right.$$

$$\left. + \frac{c_2}{\lambda T^2 [1 - \exp(-c_2/\lambda T)}\left[\Delta T_{x_0} + \frac{\rho x_0 \sin^2\alpha}{2}\int_0^1 \frac{(\Delta T_x - \Delta T_{x_0})\, x dx}{(x^2 - 2x_0 x\cos\alpha + x_0^2)^{3/2}}\right]\right\}. \tag{2}$$

The wall width of a triangular groove is taken here as unity.

The temperature profile across the height of a ring element was determined experimentally. For this purpose, at three points (at the base, in the middle, and at the vertex) of an element were welded on copper–constantan thermocouples and their readings were recorded through a model R-308 potentiometer at various temperatures of the ideal-black-body model and various ambient temperatures T_a. The results have yielded the following relation:

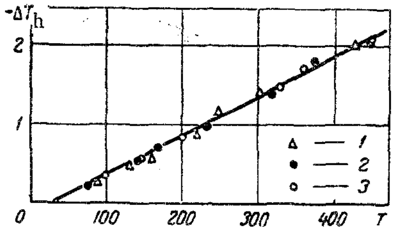

Fig. 3

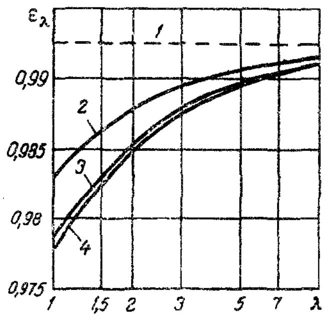

Fig. 4

Fig. 3. Temperature drop across the height of a ring element of the ideal-black-body model, T_h (°K), as a function of the ring temperature T (°K): ambient temperature T_a = 23°C (1), 26°C (2), 30°C (3).

Fig. 4. Spectral emissivity of the ideal-black-body model: isothermal model (1), real model at T = 100°C (2), real model at T = 200 and 500°C (3), real model at 300 and 400°C (4).

$$\Delta T_x = x^3 \Delta T_h = -x^3 (0.005T - 1.5). \tag{3}$$

The straight line in Fig. 3 represents Eq. (3), the test points indicated here by dots. Substituting (3) for ΔT_{x_0} and ΔT_x in the integral in (2) yields the following expression for the last term inside the braces in (2):

$$\frac{c_2(0.005T - 1.5)}{\lambda T^2 \left[1 - \exp(-c_2/\lambda T)\right]} \left\{ \frac{\rho}{2} \left[x_0^3 (1 + 5\cos\alpha) \left(1 + \frac{\cos\alpha - x_0}{\sqrt{1 + x_0^2 - 2x_0\cos\alpha}} \right) \right.\right.$$
$$- \frac{x_0 \sin^2\alpha (1 + 5x_0\cos\alpha)}{2\sqrt{1 + x_0^2 - 2x_0\cos\alpha}} - \frac{3x_0^3}{2} (5\cos^2\alpha - 1) \left(\frac{2\cos^2\alpha - 1 - x_0\cos\alpha}{1 + x_0^2 - 2x_0\cos\alpha} \right.$$
$$\left.\left. + \cos\alpha + \sin^2\alpha \ln \frac{\sqrt{1 + x_0^2 - 2x_0\cos\alpha} + 1 - x_0\cos\alpha}{x_0(1 - \cos\alpha)} \right) \right] - x_0^3 \Bigg\} . \tag{4}$$

The reflectivity of the ring coating (black chromization plus soot) on the ideal-black-body model was determined from the emissivity of the "reference" specimen, the latter measured with the same apparatus, and was found almost constant throughout the 2-10 μm range of wavelengths at a value $\rho = (1 - \varepsilon) = 0.055$.

The calculated mean-over-the-surface of a groove (the ring model of an ideal-black-body) is shown in Fig. 4 for various operating temperatures T. The ideal-black-body model and the test specimens were projecting on the radiation receiver with an appreciable reduction, i.e., the probe pad was receiving radiation from a few ring elements, which resulted in a receiver output signal proportional to the mean emissivity of the ideal-black-body model. This had been confirmed by the constant output signal throughout the scanning of the ring elements by the probe pad.

2. Nonlinearity of the Radiation Receiver. According to the data in [9], Ge–Hg receivers retain their linearity while the incident radiant flux density on their pads varies through 4-5 orders of magnitude above the threshold level. The linearity range of PbS receivers is similar [10]. Inasmuch as the maximum variation of the output signals in our measurements did not exceed 500 times the noise level, this device evidently did not constitute a source of errors.

3. Indeterminacy of the Surface Finish of the Specimen. This is a source of errors in measurements of radiation power, also when the surface finish meets special requirements.

4. Inaccuracy of Temperature Measurements. In this method of determining the ε(λ, T) characteristics the inaccuracy of temperature measurements has no effect on the accuracy of the results, because the specimen and both standards are at the same temperature. Since the metallic specimens in our tests were not thicker than 1.5 mm, hence their emitting surfaces and the solid copper disc were at the same temperature. The values of emissivity for coated specimens referred to the temperature of the metallic substrate.

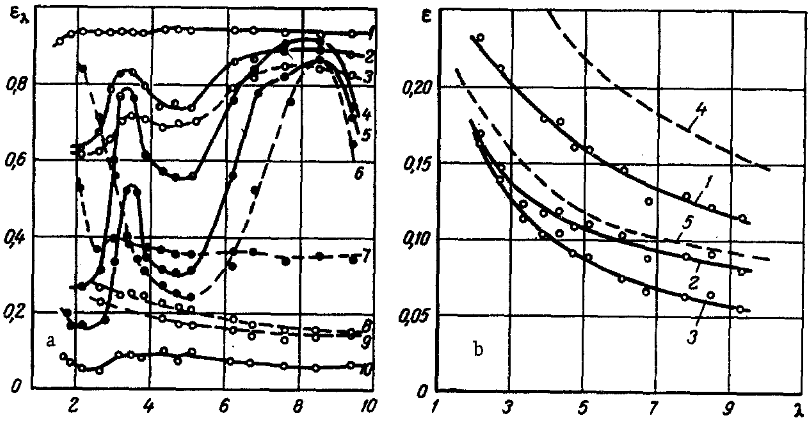

Fig. 5. Spectral emissivity of some materials; (a) coated materials, (b) titanium and nickel foils.

5. Effect of Disperse Radiation and Ambient Radiation. Since signals were recorded at the modulation frequency of the light beam, while the modulator blades were shielded by the shroud, hence the radiation from the hot yoke was thus dispersed over the components of the test apparatus and had no effect on the results of measurements. A variable modulator temperature and the ambient radiation had also no effect on the results of measurements, as had been confirmed experimentally. The modulator shroud was of such a construction as to allow cooling with vapor of liquid nitrogen and thus to facilitate measurements at modulator temperatures from room level to 0°C. Variations in the modulator temperature affected only the amplitude of recorded signals and not the values of emissivity. Owing to this, it was possible to simplify the measurement procedure and to eliminate the need for the "white" standard specimen. Since the test apparatus was shielded from local heat sources and the ambient radiation was uniform, hence, with the modulator at the ambient (room) temperature, the output signals from the radiation receiver scanning the specimen, for example, were proportional to the product of the emissivity of the scanned specimen by the difference between the energetical luminances of the ideal-black-body model at the specimen temperature and at the room temperature respectively. Thus, the magnitude of the output signals was

$$N = k\varepsilon(B^0_o - B^0_a) \text{ and } N_{bl} = k\varepsilon_{bl}(B^0_o - B^0_{amb}),$$

from which

$$\varepsilon = \varepsilon_{bl}\frac{N}{N_{bl}}. \tag{5}$$

The results of measurements according to (1) and (5) respectively agreed within the test accuracy, which indicated an almost complete absence of errors due to ambient radiation.

6. Errors due to the Difference between the Actual Radiation Wavelengths Extracted by the Optical Interference Filters and the Nominal Wavelengths. These errors did not have any decisive effect on the measurement accuracy, inasmuch as the emissivity of the test materials varied smoothly with the wavelength. An exception here were coated specimens with a characteristic radiation peak about the 3 μm level. This confirmed the close qualitative agreement between our results and those published in the technical literature for the same materials.

The use of a four-decade digital voltmeter as the recording instrument ensured a high precision in measuring the output signals of the receiver; the magnitude of random errors was determined by the signal-to-noise ratio only. The effect of random errors on the accuracy of final results was not analyzed. It is to be noted that the minimum signal-to-noise ratio in our measurements was 6.

The test results for some coated materials are shown in Fig. 5a. Pure soot burner 1 was first diluted in ethyl alcohol and then deposited with a brush on the polished surface of a copper substrate. A small amount of grade BF-2 adhesive had also been added. The finished coating was uniform and adequately wear resistant. Our data for soot agree closely with the reflectivity measurements in [11] (grade D16AT duraluminum with NKh anodization + grade KF-OZ OZh varnish + grade AK-069 varnish + grade KhV-16 varnish and total coating thickness Δ = 50 μm (2), gray percussion-grade enamel (3), grade D16AT duraluminum with colorless anodization + grade 11Z F varnish + two layers of grade AS-82 varnish and total coating thickness $\Delta = 30\ \mu m$ (4), grade V95AT duraluminum + grade AS-82 varnish at T = 200°C (5), grade D16 duraluminum chemically oxidized (6), polished copper air-oxidized (7), grade Kh18N10T steel as delivered with a $\nabla 6$ surface finish (8), grade Kh18N10T steel polished to $\nabla 7$ surface finish (9), grade V95AT duraluminum without coating at T = 200°C (10)). All test curves, except 5 and 10, correspond to a specimen temperature of 100°C. Measurements at temperatures through the 50-200°C range revealed no significant departure of $\varepsilon(\lambda, T)$ values from those curves in Fig. 5a. We also measured the emissivity of technically pure titanium and nickel foils at 200°C. The results are shown in Fig. 5b. Curve 1 represents the emissivity of tantalum foil (0.1 mm thick) as delivered. Curve 2 represents the emissivity of the same specimen after a short manual polishing treatment with diamond paste on cloth. Curve 4, taken from [13], represents the emissivity of titanium at 425°C. Curve 3 represents the emissivity of nickel as delivered and its trend is similar to that of curve 5, the latter having been obtained by an extrapolation of the data in [12] for mechanically polished polycrystalline nickel at 810°C.

On the basis of the results shown here, one may conclude that the procedure proposed by the authors for measuring the normal spectral emissivity of structural materials is sufficiently accurate and simple for use in the laboratory.

NOTATION

λ	is the wavelength;
T	is the temperature;
$\varepsilon(\lambda, T)$	is the spectral emissivity of test specimen;
$\varepsilon_{wh}(\lambda, T)$	is the spectral emissivity of "white" standard specimen;
$\varepsilon_{bl}(\lambda, T)$	is the spectral emissivity of "black" standard specimen;
N	is the magnitude of output signal from receiver scanning the test specimen;
N_{wh}	is the magnitude of output signal from receiver scanning the "white" standard;
N_{bl}	is the magnitude of output signal from receiver scanning the "black" standard;
ΔT_{x_0}, ΔT_x	are the deviations of the temperatures at points at a distance x_0 and x respectively from the vertex of a triangular groove, from the operating temperature T;
ΔT_h	is the temperature drop from vertex (x = 0) to base (x = 1) of a ring element of the ideal-black-body model;
ρ	is the reflectivity;
c_2	is the second Planck constant;
B_0^0	is the luminance of black body at the specimen temperature;
B_a^0	is the luminance of black body at the ambient temperature;
k	is the proportionality factor.

LITERATURE CITED

1. V. D. Dmitriev and G. K. Kholopov, Zh. Prikl. Spektroskopii, 3, No. 1, 72 (1965).
2. A. N. Vinnikova, V. A. Petrov, and A. E. Sheindlin, Reports from the Scientific-Technical Conf., Thermophysics Section of the Moscow Power Institute [in Russian] (1967), p. 209.
3. J. R. Grammer and E. R. Streed, Measurement of Thermal Radiation Properties of Solids, Washington D.C. (1963), p. 489.
4. P. M. Reyngolds, Brit. J. Appl. Phys., 12, No. 3, 111 (1961).
5. D. Weber, J. Opt. Soc. Amer., 49, No. 8, 815 (1959).
6. L. N. Aksyutov, A. K. Pavlyukov, and G. K. Kholopov, Inzh. Fiz. Zh., 21, No. 3, 553 (1971).
7. O. Kubashevski and E. Hopkins, Oxidation of Metals and Alloys [Russian translation], Izd. Metallurgiya, Moscow (1965).
8. A. G. Maki and E. K. Plyler, J. Res. Nat. Bur. Stand., C66, No. 3, 815 (1962).
9. Yu. A. R. Mullamaa, M. A. Sulev, V. K. Pyuldmaa, Kh. A. Okhvril', Kh. Yu. Niilisk, M. I. Allenov, L. G. Chubakov, and A. E. Kuusk, Stochastic Structure of Cloud and Radiation Fields [in Russian], Izd. Akad. Nauk ESSR, Inst. Fiz. i Astrofiz., Tartu (1971).
10. A. I. Astaf'ev and G. K. Kholopov, Opt. Mekhan. Promyshl., No. 10, 1 (1969).
11. M. A. Kropotkin and B. P. Kozyrev, Izv. LETI, No. 55, 135 (1966).
12. G. W. Autio and E. Scala, Carbon, 4, 13 (1966).
13. D. K. Edwards and N. B. deVolo, "Advances in Thermophysical Properties at Extreme Temperatures and Pressures," Proc. ASME, 74 (1965).